ACCSCIENCE PUBLISHING

Global Translational Medicine

ORIGINAL RESEARCH ARTICLE

Burden and temporal trends of cutaneous melanoma in China, 1990–2023, with projections to 2033: A systematic analysis of the Global Burden of Disease Study 2023

Benfan Lin[1] and Zhui Ke[2]*

[1]Department of Dermatology, Linyi People's Hospital, Linyi, Shandong, China

[2]Department of Oncology, Shanghai Tenth People's Hospital, Tongji University School of Medicine, Shanghai, China

Abstract

Cutaneous melanoma poses an evolving public-health challenge in China, with an epidemiological profile distinct from that of Western populations. Using data from the Global Burden of Disease Study 2023, we assessed the burden of malignant skin melanoma in China from 1990 to 2023, including prevalence, incidence, mortality, years lived with disability, years of life lost, and disability-adjusted life years (DALYs), and applied joinpoint regression, an intrinsic-estimator age–period–cohort (APC) model, and autoregressive integrated moving average (ARIMA) forecasting to 2033. Age-standardized prevalence rose from 1.39 (95% uncertainty interval [UI]: 0.82, 2.15) to 5.03 (95% UI: 3.17, 8.48) per 100,000; sex-specific prevalence rose approximately 3.38-fold in males and 2.13-fold in females, whereas mortality fell from 0.33 to 0.27 per 100,000 despite rising incidence. Period effects showed the largest variation (1.32 units for males, 0.97 for females), exceeding cohort and age effects and indicating contemporaneous factors as the principal drivers. Joinpoint analysis revealed acceleration after 2013 in males (APC 1.32% → 2.93%) and four phases in females. Sex patterns reversed by 2023, with males showing higher mortality (ratio 1.08) and DALYs (ratio 1.23), while the mortality-to-incidence ratio approximately halved in both sexes. ARIMA projected continued mortality decline (37.0% overall) through 2033, with wide long-term uncertainty. Melanoma burden in China has been transformed—markedly higher prevalence alongside falling mortality—driven predominantly by period rather than demographic effects. Interpreted in light of the acral lentiginous subtype prevalent in Chinese patients, these findings support population-specific prevention and early-detection strategies beyond ultraviolet-based paradigms.

Keywords: Melanoma; China; Global Burden of Disease; Age–period–cohort analysis; Joinpoint regression; Autoregressive integrated moving average; Mortality-to-incidence ratio; Epidemiology

***Corresponding author:**
Zhui Ke
(kezhui1314@163.com)

Citation: Lin B, Ke Z. Burden and temporal trends of cutaneous melanoma in China, 1990–2023, with projections to 2033: A systematic analysis of the Global Burden of Disease Study 2023. *Global Transl Med*. doi: 10.36922/GTM026260026

Received: June 28, 2026

Revised: August 14, 2026

Accepted: September 18, 2026

Published online: October 15, 2026

Copyright: © 2026 Author(s). This is an Open-Access article distributed under the terms of the Creative Commons Attribution License, permitting distribution, and reproduction in any medium, provided the original work is properly cited.

Publisher's Note: AccScience Publishing remains neutral with regard to jurisdictional claims in published maps and institutional affiliations.

1. Introduction

Cutaneous melanoma accounts for approximately 325,000 new cancer cases and 57,000 deaths globally each year, with incidence rates varying substantially across geographic regions and ethnic populations.[1] The disease burden has increased markedly over the past three decades, particularly in high-income countries where age-standardized incidence rates have doubled while mortality rates have remained relatively stable due to advances in early detection and treatment.[2] China presents a distinctive epidemiological profile characterized by lower overall incidence compared to Western populations yet higher case-fatality rates, reflecting differences in melanoma subtypes, diagnostic capacity, and healthcare access.

Melanoma in Chinese populations differs fundamentally from that observed in Caucasian populations. Acral lentiginous melanoma (ALM) constitutes 50%–86% of all melanomas among Chinese patients compared to less than 5% in non-Hispanic whites, with most tumors occurring on plantar surfaces, nail beds, and palmar regions rather than sun-exposed skin.[3,4] This subtype distribution challenges conventional ultraviolet (UV)-based prevention paradigms and necessitates population-specific epidemiological assessments. Previous analyses using Global Burden of Disease (GBD) data through 2017 documented an 89.2% increase in age-standardized incidence rates in China from 1990 to 2017, with particularly steep increases after 2005.[5] However, these analyses predate significant demographic transitions, including accelerated population aging, with the proportion of Chinese citizens aged 60 years and older increasing from 13.3% in 2010 to 18.7% in 2020.[6]

The temporal dynamics of melanoma burden in China remain incompletely characterized despite their importance for resource allocation and prevention planning. Recent regional comparisons identified China as having the steepest prevalence increases among East Asian countries with an average annual percentage change of 6.18%, yet the underlying drivers of these trends—whether attributable to aging demographics, birth cohort effects, or period-related factors such as improved diagnosis—have not been systematically evaluated.[7] Sex-specific patterns add another layer of complexity: international studies show that females typically have higher incidence until age 50, when patterns reverse, while males consistently exhibit worse survival outcomes across all age groups.[8] Understanding whether these patterns apply to Chinese populations requires detailed age–period–cohort (APC) decomposition using contemporary data.

Several recent analyses have examined melanoma burden in China using earlier GBD cycles: Wu *et al.*[5] reported an 89.2% rise in age-standardized incidence from 1990 to 2017 (GBD 2017); Yu *et al.*[9] mapped national and provincial burden through 2021 (GBD 2021); Xu *et al.*7 compared China with other East Asian countries over 1991–2021; and a 2025 preprint projected national burden to 2036 using joinpoint regression, decomposition, and autoregressive integrated moving average (ARIMA) on GBD 2021 data.[10] These works establish that melanoma incidence and prevalence are rising in China while mortality is stable or declining, but the drivers of these trends—whether attributable to age structure, birth-cohort exposures, or contemporaneous period factors such as improved diagnosis and treatment—have not been formally decomposed for the Chinese population, and no national analysis has yet used the GBD 2023 cycle. The present study addresses both gaps.

This study utilized GBD 2023 data to comprehensively assess melanoma burden in China from 1990 to 2023, employing joinpoint regression to identify significant trend changes, age–period–cohort models to decompose temporal effects, and ARIMA forecasting to project future burden through 2033. The GBD framework provides standardized estimates using three complementary modeling approaches—cause of death ensemble model (CODEm) for mortality, spatiotemporal Gaussian process regression (ST-GPR) for risk factors, and disease modeling–metaregression (DisMod-MR) for disease modeling—enabling robust assessment of prevalence, incidence, mortality, years lived with disability (YLDs), years of life lost (YLLs), and disability-adjusted life years (DALYs).[11] By examining 34 years of epidemiological data and projecting forward another decade, this analysis aims to inform evidence-based strategies for melanoma prevention and control within China's evolving demographic and healthcare landscape.

2. Materials and methods

2.1. Overview

Data for malignant skin melanoma in China from 1990 to 2023 were extracted from the GBD 2023 database, accessed through the Global Health Data Exchange platform (http://ghdx.healthdata.org/gbd-results-tool).[11] GBD 2023 employs multiple statistical modeling approaches, including CODEm, ST-GPR, and DisMod-MR to systematically assess disease burden across 204 countries and territories.[11,12] Six core health burden indicators were analyzed: prevalence, incidence, mortality (deaths), YLDs, YLLs, and DALYs. YLLs were calculated by multiplying the number of deaths by the standard life expectancy at the age at which death occurred. YLDs were calculated as the product of prevalence, disability weight, and duration. DALYs were calculated as the sum of YLLs and

YLDs. All rates were age-standardized using the direct standardization method with the GBD 2019 global age-standard population as the reference, covering 21 five-year age groups. Data were stratified by sex (male, female, and both sexes combined) with 95% uncertainty intervals (95% UI) generated through 1,000 Monte Carlo simulations accounting for sampling error, parameter estimation uncertainty, and data adjustment processes. As this study utilized publicly available aggregated data without individual-level identifiable information, ethical approval was not required. Throughout this article, "China" refers to the country as defined in the GBD location hierarchy—that is, the burden borne by the population resident in China—rather than to ethnically Chinese populations worldwide; consistent with the GBD hierarchy, estimates for "China" denote mainland China and do not include the special administrative regions of Hong Kong and Macao or Taiwan (Province of China), which GBD models as separate locations.

2.2. Joinpoint regression analysis

Joinpoint regression models assessed variation in incidence rate trends by identifying combinations of trends that fit the data significantly better than single-trend lines.[13] This procedure determined the number and location of joinpoints representing significant changes in temporal trends. The basic model employed a log-linear framework where $\ln(\text{Rate_t}) = \beta_0 + \beta_1 \times \text{Year_t}$, with the annual percent change calculated as $(e^{\beta} - 1) \times 100\%$. Models containing up to five joinpoints were considered, with a minimum of three observations per segment. Model selection was based on the Bayesian information criterion (BIC), calculated as $\text{BIC} = -2 \times \ln(L) + k \times \ln(n)$, where L represents the maximum likelihood value, k the number of parameters, and n the number of observations. A grid search method was employed for models with ≤ 3 joinpoints and greedy search for models with > 3 joinpoints. Statistical significance of each segment's annual percent change was tested using t-tests with the null hypothesis that annual percent change = 0, with $p < 0.05$ indicating a statistically significant non-zero trend. Analyses were stratified by sex with separate models fitted for each stratum. Joinpoint software (version 4.9.1.0; National Cancer Institute, United States of America; https://surveillance.cancer.gov/joinpoint/download) was utilized for this analysis.[13,14]

2.3. Age–period–cohort analysis

Age–period–cohort modeling using the intrinsic estimator method decomposed temporal trends in prevalence into independent age, period, and cohort effects.[15] The APC model was specified as $\log(\text{rate_ij}) = \mu + \alpha_i + \beta_j + \gamma_k$, where rate_ij represents the disease rate for age group i in period j, μ the intercept term, α_i the age effect, β_j the period effect, and γ_k the cohort effect for cohort k defined as period − age. The identification problem arising from the exact linear relationship age + cohort = period was addressed using the Moore–Penrose pseudoinverse. Parameter estimates were calculated as $\beta = (X'X)^{+} X'y$ where $(X'X)^{+}$ denotes the Moore–Penrose pseudoinverse, with standard errors calculated as $\text{SE}(\beta) = \text{sqrt}(\sigma^2 \times \text{diag}[(X'X)^{+}])$. Model fit was assessed using the R^2 coefficient of determination, Akaike information criterion (AIC), and BIC. Statistical significance of effects was tested using t-tests with $\alpha = 0.05$. For the analysis, eight five-year age groups ranging from 30–34 to 65–69 years were utilized to preserve age-specific variation needed for model estimation. R (version 4.3.2; http://www.r-project.org) and Python 3.x with relevant statistical packages were employed for model implementation.[14,15]

2.4. Autoregressive integrated moving average time series forecasting

Autoregressive integrated moving average models were developed to predict future trends from 2024 to 2033 based on historical data from 1990 to 2023.[16] The ARIMA(p, d, q) model combines autoregressive components AR(p): $Y_t = c + \varphi_1 Y_\{t-1\} + \ldots + \varphi_pY_\{t-p\} + \varepsilon_t$, integrated components with fixed $d = 2$ based on augmented Dickey–Fuller test results, and moving average components MA(q): $Y_t = \mu + \varepsilon_t + \theta_1 \varepsilon_\{t-1\} + \ldots + \theta_q\varepsilon_\{t-q\}$. Automatic model selection was performed using the pmdarima package with search ranges $p \in [0, 5]$ and $q \in [0, 5]$, minimizing $\text{AIC} = 2k - 2\ln(L)$. Model adequacy was assessed through root mean squared error (RMSE) and the Ljung–Box test for residual autocorrelation, with the null hypothesis that residuals exhibit white noise characteristics. Forecasts were generated using iterative recursive methods with confidence intervals (CIs) calculated at 90%, 95%, and 99% levels, assuming a normal distribution of forecast errors, where the 95% CI is $\hat{y}_t \pm 1.96 \times \sigma_t$, with σ_t representing the forecast standard error that increases with forecast horizon.[14,16] Second-order differencing (d = 2) was adopted because augmented Dickey–Fuller tests indicated that the level and first-differenced rate series remained non-stationary for the mortality and DALY indicators, and a common differencing order was fixed across sex strata to keep model specifications comparable; we acknowledge that this choice, applied to a short 34-point series, contributes to the wide long-horizon prediction intervals discussed in the limitations.

2.5. Data visualization and quality control

All data processing and visualization were performed using Python 3.x with pandas for data manipulation, numpy for

numerical computation, scipy and statsmodels for statistical testing, pmdarima for ARIMA modeling, and matplotlib/seaborn for graphics generation. Figures were generated in PDF vector format at 300 DPI resolution with the Arial font family on a white background. Quality control measures included verifying time series completeness, validating numerical values within reasonable ranges, testing residual normality, assessing model assumptions, and comparison with published literature trends. Statistical significance was set at $\alpha = 0.05$ (two-sided) for all tests, with 95% CIs and UIs reported throughout.

3. Results

3.1. Descriptive analysis

In 1990, the age-standardized prevalence rate of malignant skin melanoma in China was 1.39 per 100,000 population (95% UI: 0.82, 2.15), with 15,401 prevalent cases (95% UI: 9,085, 23,718); incidence of 0.49 per 100,000 (95% UI: 0.33, 0.69) with 4,657 new cases (95% UI: 3,078, 6,587); and mortality of 0.33 per 100,000 (95% UI: 0.21, 0.45) with 2,835 deaths (95% UI: 1,849, 3,860). The total disease burden was 9.74 DALYs per 100,000 (95% UI: 6.36, 13.17) or 98,386 DALYs (95% UI: 63,585, 132,734), comprising YLDs of 0.15 per 100,000 (95% UI: 0.08, 0.26) and YLLs of 9.59 per 100,000 (95% UI: 6.20, 12.96). Sex-specific patterns revealed higher age-standardized prevalence in females (1.73 per 100,000, 95% UI: 0.94, 3.15) than in males (1.05 per 100,000, 95% UI: 0.50, 1.70), with male-to-female ratios of 0.61 for prevalence, 0.80 for incidence, 0.91 for mortality, 0.72 for YLDs, 0.95 for YLLs, and 0.94 for DALYs. YLLs accounted for 98.5% of total DALYs, indicating that premature mortality, rather than disability, primarily drove the disease burden (Table 1).

By 2023, the age-standardized prevalence rate increased markedly to 5.03 per 100,000 (95% UI: 3.17, 8.48) with 102,526 cases (95% UI: 64,068, 173,695); incidence rose to 0.79 per 100,000 (95% UI: 0.54, 1.25) with 16,593 new cases (95% UI: 11,365, 26,288); while mortality decreased to 0.27 per 100,000 (95% UI: 0.19, 0.39) with 5,846 deaths (95% UI: 4,209, 8,497). DALYs declined to 7.57 per 100,000 (95% UI: 5.42, 11.14) or 158,133 DALYs total (95% UI: 113,814, 233,179), with YLDs increasing to 0.34 per 100,000 (95% UI: 0.19, 0.63) and YLLs decreasing to 7.22 per 100,000 (95% UI: 5.17, 10.64). Females maintained higher age-standardized prevalence (5.42 versus 4.60 per 100,000) though the male-to-female ratio increased to 0.85; mortality patterns reversed with males showing slightly higher rates (0.28 versus 0.26 per 100,000, ratio 1.08); males demonstrated higher burden for YLLs (7.98 versus 6.40 per 100,000, ratio 1.25) and DALYs (8.30 versus 6.75 per 100,000, ratio 1.23). YLLs remained the predominant contributor, accounting for 95.5% of total DALYs, whereas the proportion attributable to YLDs increased to 4.5% (Table 2).

Between 1990 and 2023, age-standardized prevalence rates increased 3.38-fold in males (from 1.05 to 4.60 per 100,000) and 2.13-fold in females (from 1.73 to 5.42 per 100,000), representing the largest relative increases among all indicators examined. Incidence rates increased by 76.7% in males and 51.9% in females; mortality decreased

Table 1. Baseline health burden from malignant skin melanoma in China, 1990

Measure	All-ages cases (number)			Age-standardized rates per 100,000 people		
	Male	Female	Both	Male	Female	Both
Prevalence	5,883.90 (2,777.31, 9,506.70)	9,517.08 (5,169.27, 17,084.16)	15,400.98 (9,085.48, 23,718.33)	1.05 (0.50, 1.70)	1.73 (0.94, 3.15)	1.39 (0.82, 2.15)
Incidence	2,070.82 (1,026.99, 3,153.54)	2,586.41 (1,532.19, 4,266.97)	4,657.22 (3,078.41, 6,586.89)	0.43 (0.22, 0.66)	0.54 (0.32, 0.91)	0.49 (0.33, 0.69)
Deaths	1,337.63 (667.23, 2,124.03)	1,497.19 (849.11, 2,619.66)	2,834.82 (1,848.81, 3,860.36)	0.31 (0.16, 0.49)	0.34 (0.19, 0.59)	0.330 (0.21, 0.45)
YLDs	657.45 (295.98, 1,121.86)	885.68 (416.55, 1,581.54)	1,543.13 (784.64, 2,540.65)	0.13 (0.06, 0.22)	0.18 (0.08, 0.32)	0.15 (0.08, 0.26)
YLLs	47,850.92 (23,355.44, 75,188.96)	48,991.55 (27,762.10, 83,476.89)	96,842.47 (62,081.84, 130,596.00)	9.28 (4.60, 14.62)	9.82 (5.59, 16.98)	9.59 (6.20, 12.96)
DALYs	48,508.38 (23,664.61, 75,946.58)	49,877.22 (28,316.84, 85,148.63)	98,385.60 (63,584.53, 132,734.14)	9.41 (4.67, 14.79)	9.99 (5.71, 17.25)	9.74 (6.36, 13.17)

Notes: Data presented as all-ages case numbers and age-standardized rates per 100,000 population for prevalence, incidence, mortality, YLDs, YLLs, and DALYs stratified by sex. Values in parentheses are 95% uncertainty intervals.
Abbreviations: DALYs: Disability-adjusted life years; YLLs: Years of life lost; YLDs: Years lived with disability.

by 9.7% in males and 23.5% in females; YLDs increased 1.46-fold in males and doubled in females; YLLs decreased by 14.0% in males and 34.8% in females; DALYs decreased by 11.8% in males and 32.4% in females. From 1990 to 2023, all indicators showed sex-specific trajectories, with prevalence and incidence increasing while mortality and overall disease burden declined (Figure 1; **Supplementary Table S1**).

Table 2. Current health burden from malignant skin melanoma in China, 2023

Measure	All-ages cases (number)			Age-standardized rates per 100,000 people		
	Male	Female	Both	Male	Female	Both
Prevalence	47,015.59 (27,553.86, 80,153.67)	55,510.25 (30,352.65, 106,027.35)	102,525.84 (64,067.51, 173,695.41)	4.60 (2.70, 7.84)	5.42 (3.00, 10.27)	5.03 (3.17, 8.48)
Incidence	7,799.77 (4,546.59, 12,701.70)	8,792.94 (4,997.93, 16,139.97)	16,592.71 (11,364.71, 26,288.43)	0.76 (0.44, 1.24)	0.82 (0.47, 1.50)	0.79 (0.54, 1.25)
Deaths	2,872.03 (1,709.23, 4,635.06)	2,974.14 (1,735.78, 4,800.89)	5,846.17 (4,208.65, 8,497.41)	0.28 (0.16, 0.44)	0.26 (0.15, 0.42)	0.27 (0.19, 0.39)
YLDs	3,320.07 (1,697.49, 5,504.07)	3,748.10 (1,823.35, 7,679.68)	7,068.17 (3,914.05, 12,996.65)	0.32 (0.17, 0.54)	0.36 (0.17, 0.74)	0.34 (0.19, 0.63)
YLLs	82,189.23 (49,402.27, 131,607.27)	68,875.39 (39,511.45, 112,835.77)	151,064.62 (108,916.49, 223,071.96)	7.98 (4.68, 12.81)	6.40 (3.66, 10.46)	7.22 (5.17, 10.64)
DALYs	85,509.31 (51,326.85, 136,865.57)	72,623.49 (41,870.34, 119,961.86)	158,132.80 (113,814.49, 233,178.88)	8.30 (4.88, 13.32)	6.75 (3.89, 11.19)	7.57 (5.42, 11.14)

Notes: Data presented as all-ages case numbers and age-standardized rates per 100,000 population for prevalence, incidence, mortality, YLDs, YLLs, and DALYs stratified by sex. Values in parentheses are 95% uncertainty intervals.
Abbreviations: DALYs: Disability-adjusted life years; YLLs: Years of life lost; YLDs: Years lived with disability.

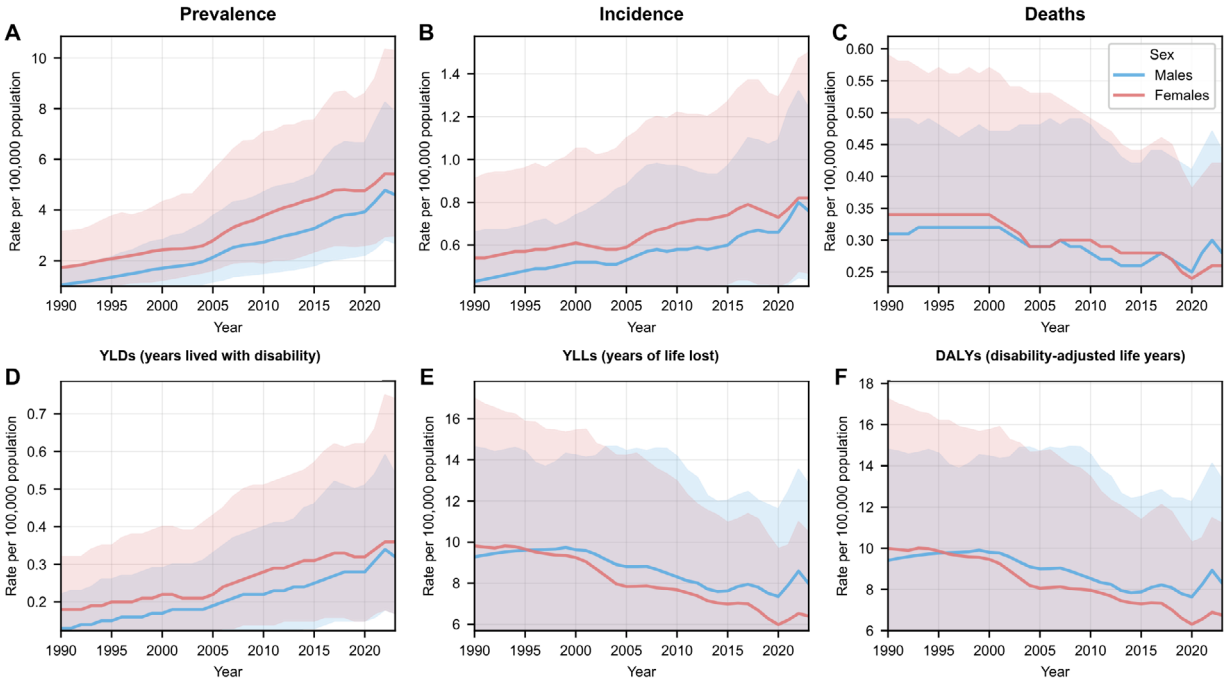


Figure 1. Temporal trends of malignant skin melanoma health metrics in China, 1990–2023. The y-axis represents age-standardized rates per 100,000 population, whereas the x-axis represents years. Blue lines indicate males, coral red lines indicate females, with shaded areas showing 95% uncertainty intervals. The six panels display (A) prevalence rate, (B) incidence rate, (C) death rate, (D) years lived with disability (YLDs), (E) years of life lost (YLLs), and (F) disability-adjusted life years (DALYs).

3.2. Joinpoint regression analysis

Joinpoint regression identified one significant change point for males in 2013 (BIC = −6.93), three for females at 2002, 2017, and 2020 (BIC = −7.29), and three for both sexes combined at 2000, 2006, and 2019 (BIC = −7.32). Male incidence showed two phases: +1.32% ($p < 0.0001$) from 1990 to 2013, accelerating to +2.93% ($p < 0.0001$) from 2013 to 2023. Female patterns showed greater complexity with four phases: +0.97% ($p < 0.0001$) from 1990 to 2002, +2.14% ($p < 0.0001$) from 2002 to 2017, −2.60% ($p < 0.0001$) from 2017 to 2020 representing the only declining segment, and +4.20% ($p = 0.0530$) from 2020 to 2023. Combined analysis revealed +1.39% ($p < 0.0001$) from 1990 to 2000, +0.50% ($p = 0.3070$) from 2000 to 2006 as the only non-significant segment, +1.43% ($p < 0.0001$) from 2006 to 2019, and the sharpest increase of +3.95% ($p = 0.0314$) from 2019 to 2023 (Figure 2; Table 3; **Supplementary Table S2**).

3.3. Age–period–cohort effects

Age–period–cohort models explained 99.49% of variance for males ($R^2 = 0.9949$, AIC = −637.03, BIC = −233.18) and 99.40% for females ($R^2 = 0.9940$, AIC = −660.20, BIC = −256.35). Age effects ranged from −0.2987 to 0.6613 for males, with the highest risk in the 55–59 years group, and from −0.2822 to 0.6042 for females, with the highest risk in the 65–69 years group; all eight age groups were statistically significant for both genders. Period effects demonstrated the largest variation (males: −0.5841 to 0.7342; females: −0.4105 to 0.5632), with 32/34 significant for males and 33/34 for females, showing consistent increases from 1990 to 2023. Cohort effects ranged from −0.3412 to 0.2602 for males (59/69 cohorts significant), and −0.4398 to 0.2448 for females (53/69 significant); the 1923–1927 birth cohort showed the lowest risk, while 1960s cohorts exhibited the highest risk for both genders. Period effects exhibited the largest variation range (males: 1.3183 units; females: 0.9737 units) compared to cohort effects (males: 0.6014; females: 0.6846) and age effects (males: 0.9600; females: 0.8864), indicating period-related factors as primary drivers of prevalence trends (Figure 3; Table 4; **Supplementary Table 3**).

3.4. Mortality-to-incidence ratio

To approximate temporal change in case fatality independent of the divergent incidence and mortality trends, we computed the mortality-to-incidence ratio (MIR; age-standardized mortality rate divided by age-standardized incidence rate) for each year. The MIR declined steadily and near-monotonically in both sexes over the study period, falling from 0.72 to 0.37 in males (a 48.9% reduction) and from 0.63 to 0.32 in females (a 49.6% reduction) between 1990 and 2023—an approximate halving consistent with substantially improved survival. Males exhibited a higher MIR than females in every year of the series, indicating persistently less favorable outcomes despite parallel improvement (Figure 4; **Supplementary Table S4**). The MIR is, however, only a surrogate for survival rather than a direct measurement: it is additionally influenced by case detection, completeness of registration, and incidence ascertainment, so its decline is best read as consistent with—but not proof of—improved survival.

3.5. Autoregressive integrated moving average forecasting

Autoregressive integrated moving average models were fitted with optimal specifications of (0,2,0) for male deaths (AIC = −186.38, RMSE = 0.06), (1,2,1) for female deaths (AIC = −221.87, RMSE = 0.07), and (0,2,0) for combined deaths (AIC = −209.82, RMSE = 0.06); all Ljung–Box tests yielded $p > 0.65$, confirming adequate fit. Mortality forecasts projected decreases from 0.3 to 0.1 per 100,000 (95% CI: −0.4, 0.6) for males representing 71.4% reduction, 0.3 to 0.2 per 100,000 (95% CI: 0.2, 0.3) for females with 8.0% reduction, and 0.3 to 0.2 per 100,000 (95% CI: −0.2, 0.5) for both sexes with 37.0% reduction by 2033. DALYs were projected to decline 75.9% for males (from 8.3 to 2.0 per 100,000, 95% CI: −9.2, 13.2), 51.7% for females (from 6.8 to 3.3 per 100,000, 95% CI: −5.3, 11.8), and 48.9% for both sexes (from 7.6 to 3.9 per 100,000, 95% CI: −4.7, 12.4). Incidence projections showed divergent patterns: an 8.4% increase for males, stable rates for females (0.0% change), and an 8.2% overall increase by 2033. Confidence intervals progressively widened from near-term (2024–2026) to long-term (2031–2033) forecasts, with some 95% prediction intervals spanning negative to positive values for mortality and DALY estimates. Because age-standardized rates cannot fall below zero, these negative lower bounds at distant horizons reflect the limitations of linear extrapolation rather than plausible values. Accordingly, the near-term forecasts (2024–2026) should be interpreted as more reliable than the long-term projections (Figure 5; Table 5; **Supplementary Table S5**).

4. Discussion

This comprehensive analysis of melanoma burden in China from 1990 to 2023 reveals a paradoxical epidemiological pattern: substantially increased prevalence (a 2.62-fold increase overall) alongside decreased mortality (−18.2%), with period effects emerging as the dominant temporal driver and sex-specific trajectories converging over time. The age-standardized prevalence rate increased from 1.39 to 5.03 per 100,000 population, driven primarily by improved diagnostic capabilities, enhanced

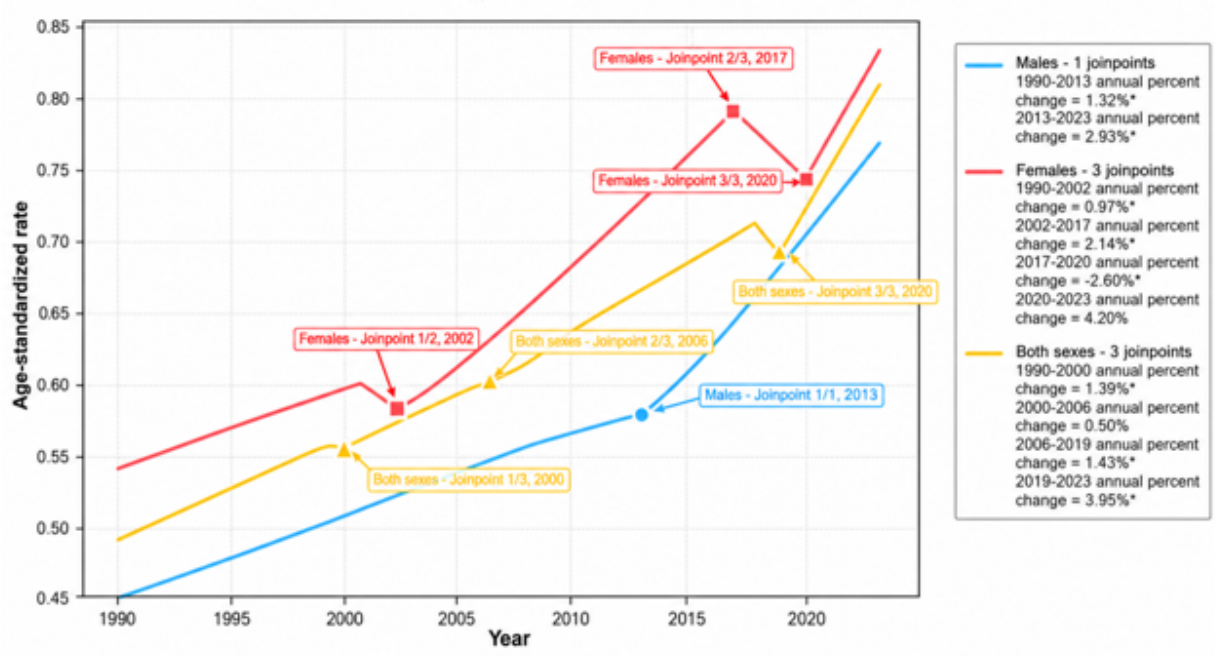


Figure 2. Joinpoint regression analysis of age-standardized incidence rates for malignant skin melanoma in China, 1990–2023. The blue line represents males with one joinpoint (2013), the red line represents females with three joinpoints (2002, 2017, 2020), whereas the yellow line represents both sexes with three joinpoints (2000, 2006, 2019). Diamond markers indicate joinpoint locations. Annual percent change values are displayed for each segment, with asterisks (*) indicating statistical significance at $p < 0.05$.

Table 3. Joinpoint regression analysis of age-standardized incidence rates of malignant skin melanoma in China, 1990–2023

Sex	Period	Annual percent change (95% CI)	AAPC (95% CI)
Both sexes	1990–2000	1.4 (1.2, 1.5)	1.4 (1.3, 1.5)
	2000–2006	0.5 (−0.4, 1.4)	
	2006–2019	1.4 (1.2, 1.7)	
	2019–2023	4.0 (1.9, 6.0)	
Males	1990–2013	1.3 (1.2, 1.4)	1.5 (1.4, 1.7)
	2013–2023	2.9 (2.2, 3.6)	
Females	1990–2002	1.0 (0.8, 1.2)	1.3 (1.2, 1.4)
	2002–2017	2.1 (1.9, 2.4)	
	2017–2020	−2.6 (−2.6, −2.6)	
	2020–2023	4.2 (2.2, 6.2)	

Notes: Annual percent change (APC) with 95% confidence intervals (CIs) for each identified trend segment, and the average annual percent change (AAPC) over the full period, stratified by sex. Joinpoint regression analysis was used to identify significant change points in temporal trends. AAPC represents the average trend over the entire study period.

healthcare access particularly in eastern provinces, and demographic aging that increased the at-risk population by approximately 200 million individuals aged over 60 years.[6,9] Our finding that period effects showed the largest variation (1.32 units for males, 0.97 units for females) compared to cohort (0.60, 0.68) and age effects (0.96, 0.89) aligns with methodological expectations from the intrinsic estimator approach, which attributes contemporaneous changes in diagnostic technology, healthcare policy, and clinical practice patterns to period rather than cohort influences.[15]

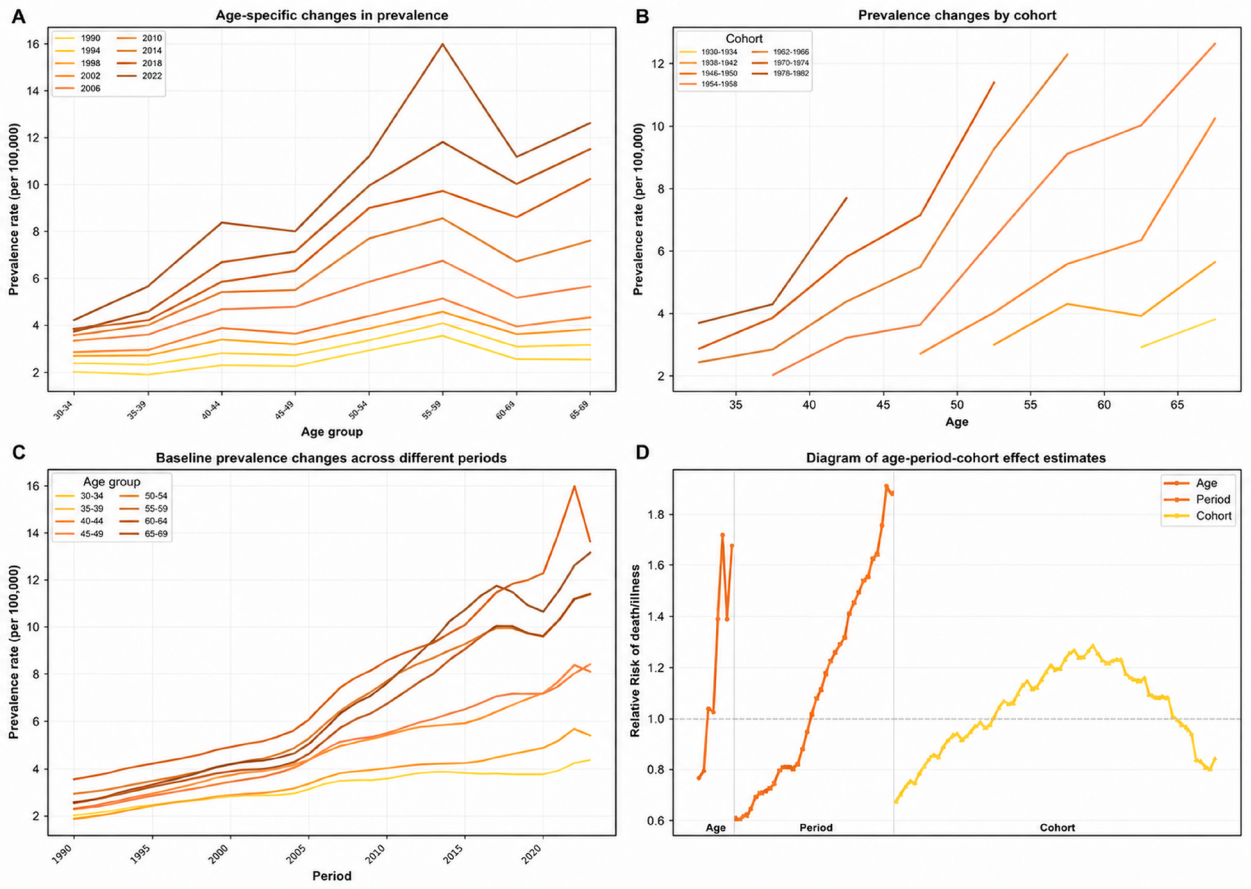


Figure 3. Age–period–cohort model decomposition of malignant skin melanoma prevalence in China. (A) Age-specific prevalence rates across different calendar periods from 1990 to 2023; (B) prevalence changes by birth cohort for ages 30–69 years; (C) period effects showing baseline prevalence changes stratified by age groups; (D) relative risk estimates for age, period, and cohort effects with 95% confidence intervals, where the dashed line at 1.0 indicates the null value. The color gradient represents temporal progression from yellow (earlier) to brown (later periods).

Table 4. Summary of the age–period–cohort model of malignant skin melanoma prevalence in China, 1990–2023

Sex	Age effect range	Period effect range	Cohort effect range	Model fit (R^2)
Males	−0.299 to 0.661	−0.584 to 0.734	−0.341 to 0.260	0.9949
Females	−0.282 to 0.604	−0.411 to 0.563	−0.440 to 0.245	0.9940

Note: The age–period–cohort model was fitted using the intrinsic estimator method. Effects represent log-scale coefficients; age groups: 30–34 years to 65–69 years; period: 1990–2023; cohort: birth years calculated from period minus age; R^2 indicates the proportion of variance explained by the model. Complete effect estimates with standard errors and p-values are available in **Supplementary Table S3**.

Our findings extend a growing body of GBD-based analyses of melanoma in China and, we contend, contribute beyond an incremental data update. Earlier reports using GBD 2017[5] and GBD 2021[7,9], along with a 2025 preprint projecting to 2036[10], consistently document rising incidence alongside stable or falling mortality, in agreement with our descriptive results. Our contribution is complementary rather than duplicative on three counts. First, we use the most recent GBD 2023 cycle and extend observation to 2023, updating the projection baseline. Second, and most importantly, our analysis reaches a different mechanistic conclusion from the most directly comparable prior work: the 2025 preprint's Das Gupta decomposition attributed the rising burden chiefly to population aging[10], whereas our intrinsic-estimator APC model localizes the dominant driver of the prevalence

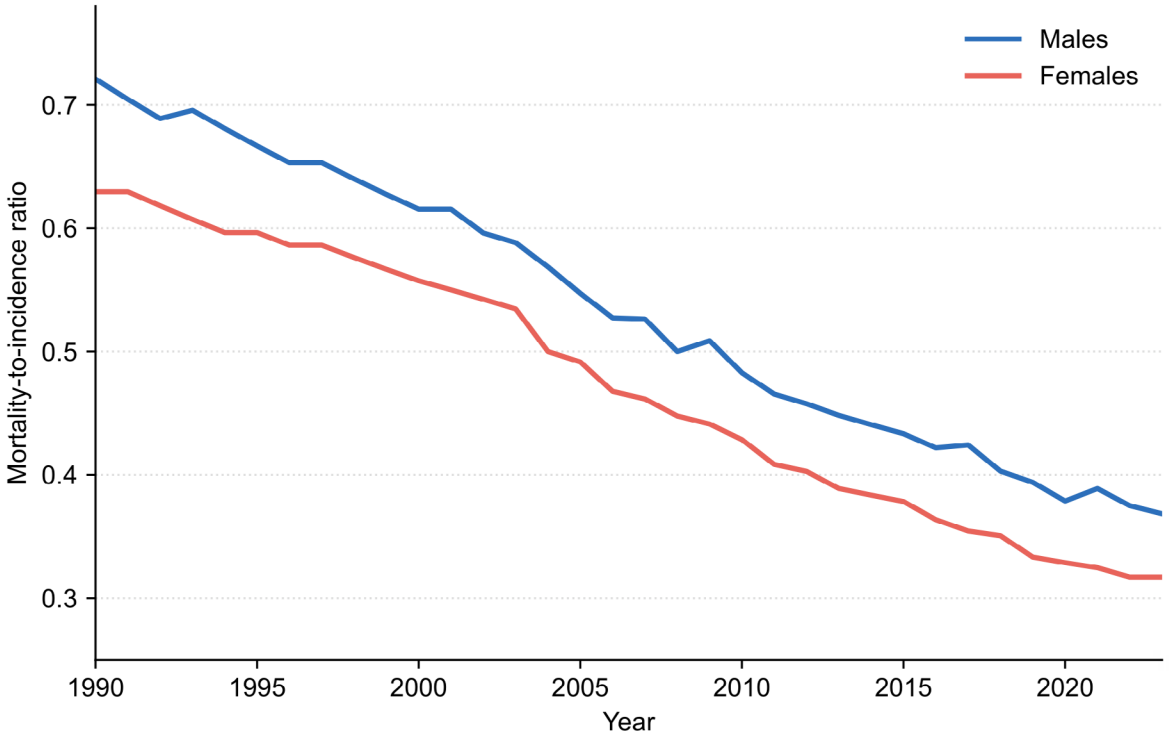


Figure 4. Mortality-to-incidence ratio (MIR) of malignant skin melanoma in China, 1990–2023. The MIR (age-standardized mortality rate divided by age-standardized incidence rate) is shown by sex, with blue indicating males and coral red indicating females. A declining ratio reflects improving survival relative to disease occurrence.

rise to period effects rather than cohort or age effects, pointing to contemporaneous diagnostic and therapeutic change rather than demographic aging as the principal force. This divergence is not merely methodological—the decomposition and provincial-mapping approaches in prior work are not designed to separate period from cohort influences—and it carries a concrete policy implication, since an aging-driven rise would imply demographic inevitability, whereas a period-driven rise implicates modifiable diagnostic and treatment practices. Third, we link this period predominance and the convergence of sex-specific trajectories to the acral lentiginous subtype that predominates in Chinese patients, yielding prevention implications beyond the UV-based paradigm. We do not provide the provincial stratification of Yu *et al.*[9] or the cross-national comparison of Xu *et al.*[7]; integrating subnational and period–cohort perspectives is a natural direction for future work.

The divergent incidence and mortality trajectories observed in our study—with incidence increasing 61.2% while mortality decreased 18.2%—reflect fundamental shifts in melanoma detection and treatment that have transformed the disease landscape over the past decade. Similar patterns have emerged across multiple healthcare systems where immunotherapy adoption has dramatically altered survival outcomes, with 10-year overall survival for metastatic melanoma improving from less than 10% before 2011 to 43% with combination immunotherapy, while early-stage detection through dermoscopy and digital surveillance has shifted stage distribution toward more favorable presentations.[17,18] This improvement is captured directly by the MIR, which approximately halved in both sexes between 1990 and 2023 (males 0.72 to 0.37; females 0.63 to 0.32), providing a survival-proxy measure that is robust to the opposing directions of the incidence and mortality trends; the consistently higher male MIR throughout the period parallels the male predominance in mortality and DALYs that emerged by 2023. The acceleration in incidence rates after 2013 identified through joinpoint regression (annual percent change increasing from 1.32% to 2.93% for males) coincides temporally with China's healthcare reforms that expanded insurance coverage from 30% to over 95% of the population between 2009 and 2015, suggesting that improved access to dermatological services may have uncovered a substantial

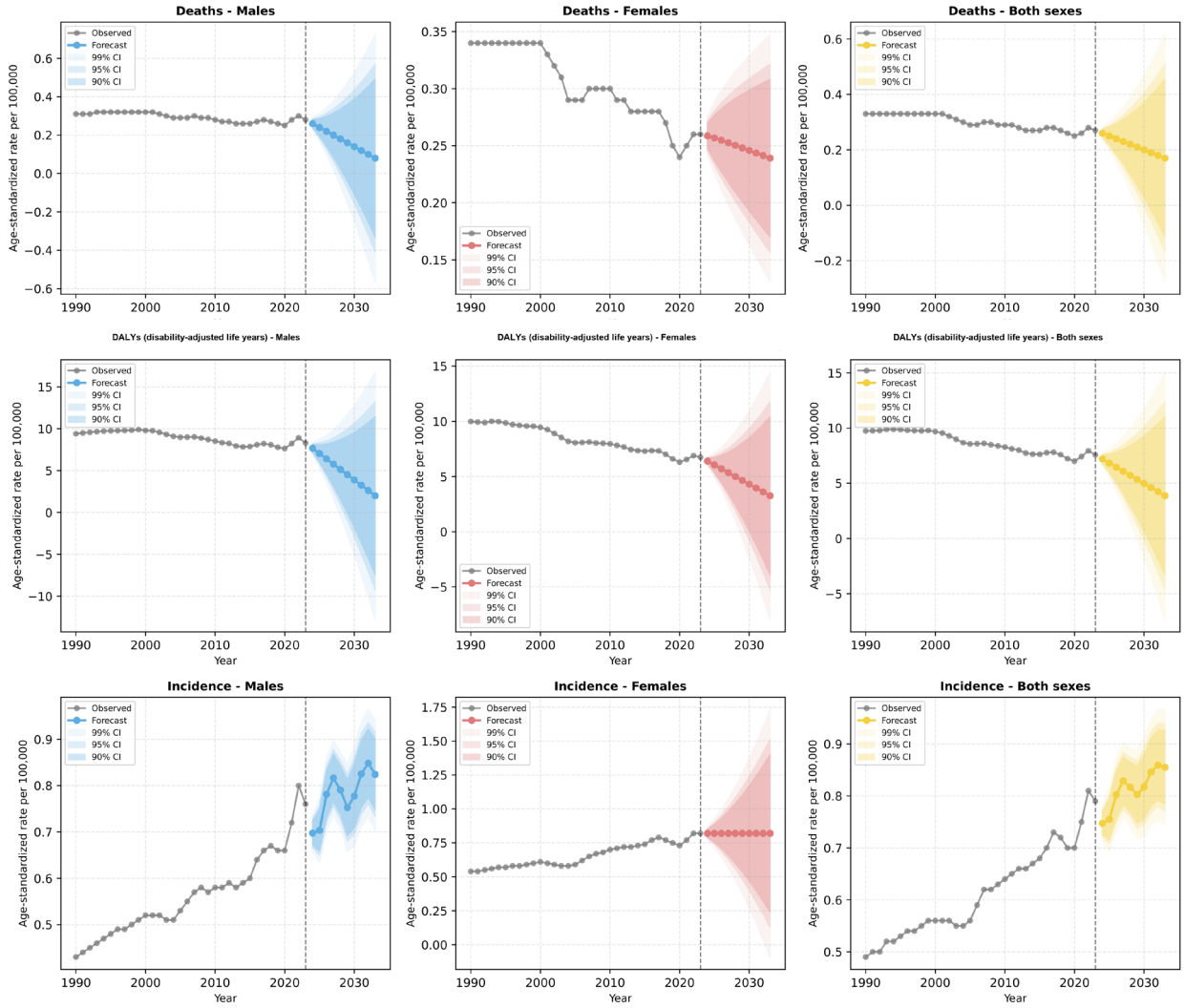


Figure 5. Autoregressive integrated moving average forecasts of malignant skin melanoma mortality, disease burden, and incidence in China, 2024–2033. Gray dotted lines represent observed historical data (1990–2023), whereas colored solid lines show point forecasts (blue for males, coral red for females, yellow for both sexes). Shaded regions indicate 90%, 95%, and 99% confidence intervals. The vertical dashed line separates historical from forecast periods. Panels display deaths (top row), DALYs (middle row), and incidence (bottom row) stratified by sex.

reservoir of previously undiagnosed cases, particularly among rural populations who historically faced significant barriers to speciality care.[19] The joinpoints identified here should not be over-interpreted as abrupt biological events. Because melanoma incidence in China is low, the annual age-standardized rates have wide UIs, and some apparent breaks — particularly short segments such as the transient decline in females between 2017 and 2020—may reflect statistical variability and modeling artifacts in the underlying GBD estimates rather than genuine inflections. Where a break coincides with an identifiable event, we note the temporal association without inferring causation: the male acceleration after 2013 follows the 2009–2015 expansion of insurance coverage, whereas the transient female decline around 2017–2020 and its subsequent rebound overlap the COVID-19 pandemic's documented disruption of cancer diagnosis and registration.

Sex-specific patterns in our analysis show a complex epidemiological transition in which the traditional female predominance in younger age groups (male-to-female ratio 0.61 for prevalence in 1990) has evolved toward male predominance in mortality and disease burden by 2023 (ratio 1.08 for mortality, 1.23 for DALYs). This epidemiological crossover, occurring around age 50–55

Table 5. ARIMA forecasts of malignant skin melanoma death rates, DALYs, and incidence in China, 2024–2033

Measure	Sex	Year	Forecast (95% CI)	Forecast (90% CI)
Deaths	Males	2024	0.3 (0.2, 0.3)	0.3 (0.2, 0.3)
Deaths	Males	2025	0.2 (0.2, 0.3)	0.2 (0.2, 0.3)
Deaths	Males	2026	0.2 (0.1, 0.3)	0.2 (0.1, 0.3)
Deaths	Males	2027	0.2 (0.1, 0.3)	0.2 (0.1, 0.3)
Deaths	Males	2028	0.2 (−0.0, 0.4)	0.2 (0.0, 0.3)
Deaths	Males	2029	0.2 (−0.1, 0.4)	0.2 (−0.0, 0.4)
Deaths	Males	2030	0.1 (−0.2, 0.4)	0.1 (−0.1, 0.4)
Deaths	Males	2031	0.1 (−0.2, 0.5)	0.1 (−0.2, 0.4)
Deaths	Males	2032	0.1 (−0.3, 0.5)	0.1 (−0.3, 0.5)
Deaths	Males	2033	0.1 (−0.4, 0.6)	0.1 (−0.3, 0.5)
Deaths	Females	2024	0.3 (0.2, 0.3)	0.3 (0.2, 0.3)
Deaths	Females	2025	0.3 (0.2, 0.3)	0.3 (0.2, 0.3)
Deaths	Females	2026	0.3 (0.2, 0.3)	0.3 (0.2, 0.3)
Deaths	Females	2027	0.3 (0.2, 0.3)	0.3 (0.2, 0.3)
Deaths	Females	2028	0.3 (0.2, 0.3)	0.3 (0.2, 0.3)
Deaths	Females	2029	0.2 (0.2, 0.3)	0.2 (0.2, 0.3)
Deaths	Females	2030	0.2 (0.2, 0.3)	0.2 (0.2, 0.3)
Deaths	Females	2031	0.2 (0.2, 0.3)	0.2 (0.2, 0.3)
Deaths	Females	2032	0.2 (0.2, 0.3)	0.2 (0.2, 0.3)
Deaths	Females	2033	0.2 (0.2, 0.3)	0.2 (0.2, 0.3)
Deaths	Both sexes	2024	0.3 (0.2, 0.3)	0.3 (0.2, 0.3)
Deaths	Both sexes	2025	0.3 (0.2, 0.3)	0.3 (0.2, 0.3)
Deaths	Both sexes	2026	0.2 (0.2, 0.3)	0.2 (0.2, 0.3)
Deaths	Both sexes	2027	0.2 (0.1, 0.3)	0.2 (0.2, 0.3)
Deaths	Both sexes	2028	0.2 (0.1, 0.3)	0.2 (0.1, 0.3)
Deaths	Both sexes	2029	0.2 (0.0, 0.4)	0.2 (0.1, 0.3)
Deaths	Both sexes	2030	0.2 (−0.0, 0.4)	0.2 (0.0, 0.4)
Deaths	Both sexes	2031	0.2 (−0.1, 0.4)	0.2 (−0.0, 0.4)
Deaths	Both sexes	2032	0.2 (−0.1, 0.5)	0.2 (−0.1, 0.4)
Deaths	Both sexes	2033	0.2 (−0.2, 0.5)	0.2 (−0.1, 0.5)
DALYs	Males	2024	7.7 (7.1, 8.2)	7.7 (7.2, 8.2)
DALYs	Males	2025	7.0 (5.8, 8.3)	7.0 (6.0, 8.1)
DALYs	Males	2026	6.4 (4.3, 8.6)	6.4 (4.6, 8.2)
DALYs	Males	2027	5.8 (2.6, 8.9)	5.8 (3.1, 8.4)
DALYs	Males	2028	5.1 (0.9, 9.4)	5.1 (1.6, 8.7)
DALYs	Males	2029	4.5 (−0.9, 10.0)	4.5 (−0.1, 9.1)
DALYs	Males	2030	3.9 (−2.9, 10.7)	3.9 (−1.8, 9.6)
DALYs	Males	2031	3.3 (−4.9, 11.4)	3.3 (−3.6, 10.1)
DALYs	Males	2032	2.6 (−7.0, 12.3)	2.6 (−5.5, 10.8)
DALYs	Males	2033	2.0 (−9.2, 13.2)	2.0 (−7.4, 11.4)

(*Cont'd...*)

Table 5. (***Continued***)

Measure	Sex	Year	Forecast (95% CI)	Forecast (90% CI)
DALYs	Females	2024	6.4 (6.1, 6.7)	6.4 (6.1, 6.7)
DALYs	Females	2025	6.1 (5.2, 6.9)	6.1 (5.4, 6.7)
DALYs	Females	2026	5.7 (4.2, 7.2)	5.7 (4.5, 6.9)
DALYs	Females	2027	5.4 (3.1, 7.6)	5.4 (3.5, 7.2)
DALYs	Females	2028	5.0 (1.9, 8.1)	5.0 (2.4, 7.6)
DALYs	Females	2029	4.7 (0.6, 8.7)	4.7 (1.3, 8.0)
DALYs	Females	2030	4.3 (−0.7, 9.3)	4.3 (0.1, 8.5)
DALYs	Females	2031	4.0 (−2.2, 10.1)	4.0 (−1.2, 9.1)
DALYs	Females	2032	3.6 (−3.7, 10.9)	3.6 (−2.5, 9.7)
DALYs	Females	2033	3.3 (−5.3, 11.8)	3.3 (−3.9, 10.4)
DALYs	Both sexes	2024	7.2 (6.8, 7.6)	7.2 (6.8, 7.6)
DALYs	Both sexes	2025	6.8 (5.9, 7.8)	6.8 (6.0, 7.6)
DALYs	Both sexes	2026	6.5 (4.8, 8.1)	6.5 (5.1, 7.8)
DALYs	Both sexes	2027	6.1 (3.7, 8.5)	6.1 (4.1, 8.1)
DALYs	Both sexes	2028	5.7 (2.5, 8.9)	5.7 (3.0, 8.4)
DALYs	Both sexes	2029	5.4 (1.2, 9.5)	5.4 (1.9, 8.8)
DALYs	Both sexes	2030	5.0 (−0.2, 10.1)	5.0 (0.7, 9.3)
DALYs	Both sexes	2031	4.6 (−1.6, 10.8)	4.6 (−0.6, 9.8)
DALYs	Both sexes	2032	4.2 (−3.1, 11.6)	4.2 (−1.9, 10.4)
DALYs	Both sexes	2033	3.9 (−4.7, 12.4)	3.9 (−3.3, 11.0)
Incidence	Males	2024	0.7 (0.7, 0.7)	0.7 (0.7, 0.7)
Incidence	Males	2025	0.7 (0.6, 0.8)	0.7 (0.7, 0.7)
Incidence	Males	2026	0.8 (0.7, 0.8)	0.8 (0.7, 0.8)
Incidence	Males	2027	0.8 (0.8, 0.9)	0.8 (0.8, 0.9)
Incidence	Males	2028	0.8 (0.7, 0.9)	0.8 (0.7, 0.8)
Incidence	Males	2029	0.8 (0.7, 0.8)	0.8 (0.7, 0.8)
Incidence	Males	2030	0.8 (0.7, 0.9)	0.8 (0.7, 0.8)
Incidence	Males	2031	0.8 (0.7, 0.9)	0.8 (0.8, 0.9)
Incidence	Males	2032	0.8 (0.8, 0.9)	0.8 (0.8, 0.9)
Incidence	Males	2033	0.8 (0.7, 0.9)	0.8 (0.7, 0.9)
Incidence	Females	2024	0.8 (0.8, 0.9)	0.8 (0.8, 0.8)
Incidence	Females	2025	0.8 (0.7, 0.9)	0.8 (0.8, 0.9)
Incidence	Females	2026	0.8 (0.7, 1.0)	0.8 (0.7, 0.9)
Incidence	Females	2027	0.8 (0.6, 1.0)	0.8 (0.7, 1.0)
Incidence	Females	2028	0.8 (0.6, 1.1)	0.8 (0.6, 1.0)
Incidence	Females	2029	0.8 (0.5, 1.2)	0.8 (0.5, 1.1)
Incidence	Females	2030	0.8 (0.4, 1.2)	0.8 (0.5, 1.2)
Incidence	Females	2031	0.8 (0.3, 1.3)	0.8 (0.4, 1.2)
Incidence	Females	2032	0.8 (0.2, 1.4)	0.8 (0.3, 1.3)
Incidence	Females	2033	0.8 (0.1, 1.5)	0.8 (0.2, 1.4)

(*Cont'd...*)

Table 5. (*Continued*)

Measure	Sex	Year	Forecast (95% CI)	Forecast (90% CI)
Incidence	Both sexes	2024	0.7 (0.7, 0.8)	0.7 (0.7, 0.8)
Incidence	Both sexes	2025	0.8 (0.7, 0.8)	0.8 (0.7, 0.8)
Incidence	Both sexes	2026	0.8 (0.7, 0.9)	0.8 (0.8, 0.8)
Incidence	Both sexes	2027	0.8 (0.8, 0.9)	0.8 (0.8, 0.9)
Incidence	Both sexes	2028	0.8 (0.8, 0.9)	0.8 (0.8, 0.9)
Incidence	Both sexes	2029	0.8 (0.7, 0.9)	0.8 (0.7, 0.9)
Incidence	Both sexes	2030	0.8 (0.7, 0.9)	0.8 (0.8, 0.9)
Incidence	Both sexes	2031	0.8 (0.8, 0.9)	0.8 (0.8, 0.9)
Incidence	Both sexes	2032	0.9 (0.8, 0.9)	0.9 (0.8, 0.9)
Incidence	Both sexes	2033	0.9 (0.8, 0.9)	0.9 (0.8, 0.9)

Notes: Point forecasts with 95% and 90% CIs by sex. Forecasts were generated using ARIMA models with second-order differencing (d = 2). The 95% and 90% CIs reflect forecast uncertainty. Model specifications and diagnostics are provided in **Supplementary Table S5**. Abbreviations: ARIMA: Autoregressive integrated moving average; CI: Confidence interval; DALYs: Disability-adjusted life years.

in our age-specific analysis, mirrors patterns documented across diverse populations and likely reflects the interaction of hormonal protection in premenopausal women with cumulative occupational and environmental exposures that disproportionately affect males in China's industrial workforce.[8,20] The particularly steep increase in male prevalence (3.38-fold versus 2.13-fold for females) may additionally reflect gender disparities in health-seeking behavior, with Chinese males traditionally delaying medical consultation until advanced disease stages, though recent public health campaigns have begun addressing these behavioral patterns.

The biological characteristics of melanoma in Chinese populations fundamentally differ from Western populations in ways that profoundly influence epidemiological patterns and clinical outcomes. ALM constitutes 50%–86% of cases in our population compared to less than 5% in Caucasians, with median Breslow thickness at diagnosis of 3.0 mm versus 1.0 mm and ulceration present in 66.1% versus 20% of cases, explaining the persistently high contribution of YLLs to total DALYs (95.5% in 2023) despite therapeutic advances.[3,21] These tumors arise through UV-independent pathways involving *KIT* mutations and cyclin-dependent kinase alterations rather than the *BRAF* mutations common in cutaneous melanomas; they occur predominantly on plantar surfaces exposed to chronic trauma and agricultural chemicals rather than solar radiation, which explains why traditional UV-based prevention strategies have limited applicability in Chinese populations.[4,22] The late-stage presentation characteristic of ALM, combined with its anatomical location in areas subject to delayed recognition, creates a cascade of adverse outcomes including higher surgical morbidity, reduced eligibility for sentinel node biopsy, and inferior response rates to conventional immunotherapy regimens optimized for *BRAF*-mutant tumors.

Autoregressive integrated moving average forecasting projects continued mortality decline through 2033 (37.0% reduction overall), though with substantial uncertainty reflected in confidence intervals spanning negative to positive values, highlighting the challenge of long-term projections in rapidly evolving therapeutic and demographic contexts. The divergent forecasts for incidence (8.4% increase for males, stable for females) versus mortality suggest that improvements in survival will continue outpacing increases in new cases, driven by expanding adoption of adjuvant immunotherapy, refined surgical techniques, and earlier detection through artificial intelligence-assisted dermoscopy now being deployed across major Chinese medical centers.[16] However, these optimistic projections assume continued healthcare investment and may not fully account for potential saturation effects in detection improvements or the economic sustainability of expensive immunotherapy regimens that currently cost 10–15 times the average annual disposable income in China. These forecasts should be regarded as indicative rather than precise. They rest on only 34 annual observations with second-order differencing, a combination that, together with Gaussian prediction intervals, widens long-horizon uncertainty and produces the implausible negative lower bounds noted in **Section 3**; the small "saw-tooth" oscillations visible in some forecast curves (for example, female deaths around 2030) are artifacts of the moving-average structure interacting with differencing on a short series,

fall well within the prediction intervals, and carry no biological meaning. Near-term projections (2024–2026) are therefore more reliable than distant ones. We could not validate the forecasts against observed 2024–2025 deaths because national, cause-specific melanoma mortality for those years has not yet been released; we therefore relied on in-sample diagnostics (RMSE and Ljung–Box tests) and present the projections with these caveats.

Several methodological considerations constrain the interpretation of our findings and highlight areas requiring further investigation. The GBD modeling framework, while providing standardized estimates that enable international comparisons, relies on sparse primary data for China with only 12 cancer registries covering less than 6% of the national population, potentially underestimating burden in western provinces where healthcare infrastructure remains underdeveloped.[11] Because these registries are concentrated in eastern, urban areas, the GBD estimates for China depend more heavily on statistical modeling and covariate-based imputation than in settings with comprehensive registration; this both widens uncertainty and may bias national rates toward better-covered regions, and the resulting uncertainty propagates into the APC decomposition and is carried forward and amplified by the ARIMA forecasts, so all three analyses should be interpreted with these data constraints in mind. Our APC analysis restricted to ages 30–69 years may miss important patterns in elderly populations where melanoma burden is increasing most rapidly, though this restriction was necessary to maintain model stability given the collinearity constraints inherent in APC decomposition. Furthermore, the intrinsic-estimator solution to the APC identification problem rests on a specific orthogonality constraint whose validity remains debated[15]; we therefore base our inference of period predominance on the relative magnitude of the estimated effect ranges rather than on any individual coefficient, and we regard it as indicative rather than definitive, warranting confirmation with alternative identification strategies such as net-drift estimation. The assumption of constant disability weights across the 34-year study period likely underestimates improvements in quality of life associated with modern supportive care, while our forecasting models cannot anticipate disruptive innovations such as mRNA vaccines or CAR-T cell therapy currently in clinical trials for melanoma. Regional heterogeneity within China, with coastal provinces showing incidence rates three times higher than inland regions, suggests that national-level analyses may obscure important subnational patterns requiring targeted interventions.[9] Finally, the APC model quantifies the relative magnitude of age, period, and cohort effects but cannot, by itself, identify the mechanisms that generate a period effect; our attribution of the dominant period effect to improved diagnosis and treatment is therefore a hypothesis rather than an established mechanism, and the period signal may equally reflect other contemporaneous changes such as expanding healthcare access, more complete disease registration and case ascertainment, and secular shifts in environmental or occupational exposures.

The increasing melanoma burden documented in this study necessitates comprehensive public health strategies adapted to the unique epidemiological profile of Chinese populations. Primary prevention efforts should prioritize occupational safety in agricultural and industrial settings where chemical exposures may contribute to acral melanoma risk, while public education campaigns should shift focus from sun protection to recognizing pigmented lesions on palmar and plantar surfaces where most Chinese melanomas arise.[23] Secondary prevention through early detection programs faces particular challenges given that dermoscopy has limited sensitivity for amelanotic ALM variants common in Asian populations, suggesting potential value in alternative screening modalities such as high-frequency ultrasound or confocal microscopy currently under evaluation. Healthcare system strengthening should emphasize training primary care physicians to recognize acral lesions, as early acral melanomas are frequently mistaken for benign nevi or traumatic changes and physician-related diagnostic delay is a recognized contributor to advanced-stage presentation.[24] Economic considerations argue for risk-stratified screening approaches targeting high-risk groups such as agricultural workers and individuals with multiple plantar nevi, as universal population screening would be prohibitively expensive given current dermatologist shortages and the low overall incidence compared to other cancers.

5. Conclusion

The melanoma burden in China has undergone substantial transformation from 1990 to 2023, characterized by rising prevalence driven by period effects including improved diagnosis and population aging, while mortality has declined due to therapeutic advances despite the predominance of aggressive acral lentiginous subtypes. Sex-specific trajectories have converged, with males now experiencing higher mortality and disease burden, while projections suggest continued mortality improvements through 2033, though with considerable uncertainty. These findings underscore the need for population-specific prevention and early detection strategies that account for the unique biological characteristics of melanoma in Chinese populations, alongside continued investment in healthcare infrastructure to ensure equitable access to advances in diagnosis and treatment across all provinces.

Acknowledgments

None.

Funding

This research received no specific grant from any funding agency in the public, commercial, or not-for-profit sectors.

Conflict of interest

The authors declare they have no competing interests.

Author contributions

Conceptualization: Benfan Lin, Zhui Ke
Data curation: Benfan Lin
Formal analysis: Benfan Lin
Methodology: Benfan Lin
Supervision: Zhui Ke
Validation: Zhui Ke
Visualization: Benfan Lin
Writing–original draft: Benfan Lin
Writing–review & editing: Zhui Ke

Ethics approval and consent to participate

Not applicable. This study analyzed publicly available, fully aggregated data from the Global Burden of Disease Study 2023 without individual-level identifiable information; ethical approval and informed consent to participate were not required.

Consent for publication

Not applicable.

Availability of data

The data underlying this study are openly available from the Global Health Data Exchange (GHDx) at https://ghdx.healthdata.org/gbd-results-tool.

References

1. Arnold M, Singh D, Laversanne M, *et al.* Global Burden of Cutaneous Melanoma in 2020 and Projections to 2040. *JAMA Dermatol*. 2022;158(5):495-503.

   doi:10.1001/jamadermatol.2022.0160

2. Guy GP Jr, Thomas CC, Thompson T, *et al.* Vital signs: melanoma incidence and mortality trends and projections - United States, 1982-2030. *MMWR Morb Mortal Wkly Rep*. 2015;64(21):591-596.

3. Chi Z, Li S, Sheng X, *et al.* Clinical presentation, histology, and prognoses of malignant melanoma in ethnic Chinese: a study of 522 consecutive cases. *BMC Cancer*. 2011;11(1):85.

   doi:10.1186/1471-2407-11-85

4. Gloster HM Jr, Neal K. Skin cancer in skin of color. *J Am Acad Dermatol*. 2006;55(5):741-760.

   doi:10.1016/j.jaad.2005.08.063

5. Wu Y, Wang Y, Wang L, *et al.* Burden of melanoma in China, 1990-2017: Findings from the 2017 global burden of disease study. *Int J Cancer*. 2020;147(3):692-701.

   doi:10.1002/ijc.32764

6. Zheng R, Zhang S, Zeng H, *et al.* Cancer incidence and mortality in China, 2016. *J Natl Cancer Cent*. 2022;2(1):1-9.

   doi:10.1016/j.jncc.2022.02.002

7. Xu J, Wang X, Liu W, *et al.* Analysis and comparison of the trends in burden of malignant cutaneous melanoma in East Asian countries and regions and worldwide from 1991 to 2021. *Front Public Health*. 2025;13:1487177.

   doi:10.3389/fpubh.2025.1487177

8. Joosse A, Collette S, Suciu S, *et al.* Sex is an independent prognostic indicator for survival and relapse/progression-free survival in metastasized stage III to IV melanoma: a pooled analysis of five European organisation for research and treatment of cancer randomized controlled trials. *J Clin Oncol*. 2013;31(18):2337-2346.

   doi:10.1200/JCO.2012.44.5031

9. Yu L, Yan F, Qi J, *et al.* Burden of melanoma in China and its provinces from 1990 to 2021: an analysis for the Global Burden of Disease Study 2021. *Front Public Health*. 2024;12:1486617.

   doi:10.3389/fpubh.2024.1486617

10. Zhao C, Ma K, Wu Z, *et al.* The Burden of Malignant Skin Melanoma in China: From 1990 to 2021 with Estimation to 2036. *medRxiv*. Published online August 17, 2025.

    doi:10.1101/2025.08.11.25333476

11. GBD 2019 Diseases and Injuries Collaborators. Global burden of 369 diseases and injuries in 204 countries and territories, 1990-2019: a systematic analysis for the Global Burden of Disease Study 2019. *Lancet*. 2020;396(10258):1204-1222.

    doi:10.1016/S0140-6736(20)30925-9

12. Soerjomataram I, Lortet-Tieulent J, Ferlay J, *et al.* Estimating and validating disability-adjusted life years at the global level: a methodological framework for cancer. *BMC Med Res Methodol*. 2012;12(1):125.

    doi:10.1186/1471-2288-12-125

13. Kim HJ, Fay MP, Feuer EJ, Midthune DN. Permutation tests for joinpoint regression with applications to cancer rates. *Stat Med*. 2000;19(3):335-351.

    doi:10.1002/(SICI)1097-0258(20000215)19:3<335::AID-SIM336>3.0.CO;2-Z

14. Volinsky CT, Raftery AE. Bayesian information criterion for censored survival models. *Biometrics*. 2000;56(1):256-262.

doi:10.1111/j.0006-341X.2000.00256.x

15. Yang Y, Schulhofer-Wohl S, Fu WJ, Land KC. The intrinsic estimator for age-period-cohort analysis: what it is and how to use it. *Am J Sociol*. 2008;113(6):1697-1736.

doi:10.1086/587154

16. Earnest A, Evans SM, Sampurno F, Millar J. Forecasting annual incidence and mortality rate for prostate cancer in Australia until 2022 using autoregressive integrated moving average (ARIMA) models. *BMJ Open*. 2019;9(8):e031331.

doi:10.1136/bmjopen-2019-031331

17. Wolchok JD, Chiarion-Sileni V, Gonzalez R, *et al.* Long-term outcomes with nivolumab plus ipilimumab or nivolumab alone versus ipilimumab in patients with advanced melanoma. *J Clin Oncol*. 2022;40(2):127-137.

doi:10.1200/JCO.21.02229

18. Larkin J, Chiarion-Sileni V, Gonzalez R, *et al.* Five-year survival with combined nivolumab and ipilimumab in advanced melanoma. *N Engl J Med*. 2019;381(16):1535-1546.

doi:10.1056/NEJMoa1910836

19. Ke X, Lin W, Li D, *et al.* Spending and hospital stay for melanoma in Hunan, China. *Front Public Health*. 2022;10:917119.

doi:10.3389/fpubh.2022.917119

20. Enninga EAL, Moser JC, Weaver AL, *et al.* Survival of cutaneous melanoma based on sex, age, and stage in the United States, 1992-2011. *Cancer Med*. 2017;6(10):2203-2212.

doi:10.1002/cam4.1152

21. Bradford PT, Goldstein AM, McMaster ML, Tucker MA. Acral lentiginous melanoma: incidence and survival patterns in the United States, 1986-2005. *Arch Dermatol*. 2009;145(4):427-434.

doi:10.1001/archdermatol.2008.609

22. Curtin JA, Fridlyand J, Kageshita T, *et al.* Distinct sets of genetic alterations in melanoma. *N Engl J Med*. 2005;353(20):2135-2147.

doi:10.1056/NEJMoa050092

23. Holman DM, Freeman MB, Shoemaker ML. Trends in melanoma incidence among non-Hispanic whites in the United States, 2005 to 2014. *JAMA Dermatol*. 2018;154(3):361-362.

doi:10.1001/jamadermatol.2017.5541

24. Richard MA, Grob JJ, Avril MF, *et al.* Delays in diagnosis and melanoma prognosis (II): the role of doctors. *Int J Cancer*. 2000;89(3):280-285.

doi:10.1002/1097-0215(20000520)89:3<280::AID-IJC11>3.0.CO;2-2